Surface & Coatings Technology 271 (2015) 92–99

Contents lists available at ScienceDirect

Surface & Coatings Technology

journal homepage: www.elsevier.com/locate/surfcoat

Mechanical and electrochemical properties of Nb_2O_5, Nb_2O_5:Cu and graphene layers deposited on titanium alloy (Ti6Al4V)

M. Kalisz [a,*], M. Grobelny [a], M. Mazur [b], D. Wojcieszak [b], M. Świniarski [c], M. Zdrojek [c], J. Domaradzki [b], D. Kaczmarek [b]

[a] Motor Transport Institute, Centre for Material Testing and Mechatronics, Jagiellońska 80, Warsaw, Poland
[b] Faculty of Microsystem Electronics and Photonics, Wroclaw University of Technology, Janiszewskiego 11/17, Wroclaw, Poland
[c] Faculty of Physics, Warsaw University of Technology, Koszykowa 75, 00-662 Warsaw, Poland

ARTICLE INFO

Available online 8 January 2015

Keywords:
Thin films
Magnetron sputtering
Graphene
Titanium alloys
Nanoindentation
Corrosion properties

ABSTRACT

In this paper the comparative studies on structural, mechanical and corrosion properties of Nb_2O_5/Ti, Nb_2O_5:Cu/Ti–Al–V and graphene/Ti alloy systems have been investigated. The pure nioba and nioba with copper addition were deposited on Ti6Al4V titanium alloy surface by magnetron sputtering method. Graphene monolayer was transferred on titanium alloy substrate using "PMMA-mediated" method. The structural characteristics of obtained thin films were examined by using of Raman spectroscopy, SEM and AFM measurement. The mechanical properties i.e.: nanohardness, were performed by using nanoindenter. Corrosion properties of the coatings were determined by analysis of the voltammetric curves.

The deposited Nb_2O_5 and Nb_2O_5:Cu coatings were crack free and exhibited good adherence to the substrate, no discontinuities of the thin films were observed and the surface morphology was homogeneous. Graphene transferred on titanium alloy surface was a single layer without defects.

The hardness of pure niobium pentoxide was ca. 8.64 GPa, nioba with copper addition was equal 7.79 GPa and graphene depositied on titanium alloy surface was equal 5.63 GPa. As obtained results show, graphene monolayer has no effect on surface hardness of titanium alloy. However, sample Ti6Al4V coated with a single layer of graphene is characterized by the best corrosion resistance. Similar results were obtained for the sample covered by 210 nm thick Nb_2O_5:Cu thin film.

It seems, that the combined advantages of these three layers, i.e., niobium pentoxide, niobium with copper addition and a monolayer of graphene, in the hybrid multilayer system can greatly improve the mechanical and corrosion properties of the titanium alloy surface. This hybrid system can be used in the future, as protection coatings for Ti alloy, in biomedical application and in other application, where Ti alloy works in an aggressive corrosive environment and in engineering applications where friction is involved.

1. Introduction

In the last period we observe a significant increase in the world-wide production of castings from light metal alloys such as titanium. It is associated not only with an increase in the demand for lightweight structural components in the automotive, aviation and aerospace industry, but also with an increase in interest from manufacturers of various household appliances, electronics, video cameras, mobile phones and others. Particularly rapid growth in the production of castings from titanium alloys is observed in Germany, Italy and the USA. The advantage of titanium alloys is their small specific gravity, yield strength and modulus of elasticity that allow the transfer of heavy loads. Titanium alloys because of their biocompatibility, have also become a desirable construction material for the production of medical implants. They have many potential industrial applications, but their implementation is limited due to problems with unsatisfactory surface mechanical parameters, i.e. low hardness, low wear resistance and low corrosion resistance in hot, concentrated and low-pH solutions [1,2].

To show the effect of the solution type on the corrosion properties of titanium alloys, two kinds of solutions were used and compared: i.e. neutral sodium chloride (0.5 M NaCl, pH = 5.7) and acid sodium chloride solution with the addition of fluoride ions (0.5 M NaCl, 2 g/l KF, pH = 2). Fig. 1 illustrates the effect of a kind of electrolyte on the polarization curves for Ti6Al6V titanium alloy.

The results of measurements of electrochemical parameters of the samples obtained from these curves are collected in Table 1.

The obtained results present clear evidence that the corrosion properties of titanium alloy strongly depend on the composition of the electrolyte used. The lower rate of corrosion processes expressed by the lower corrosion current i_{corr}, was observed in the neutral solution. In this kind of solution the titanium oxides may appear on the surface of

* Corresponding author.
E-mail address: malgorzata.kalisz@its.waw.pl (M. Kalisz).

http://dx.doi.org/10.1016/j.surfcoat.2015.01.002
0257-8972/

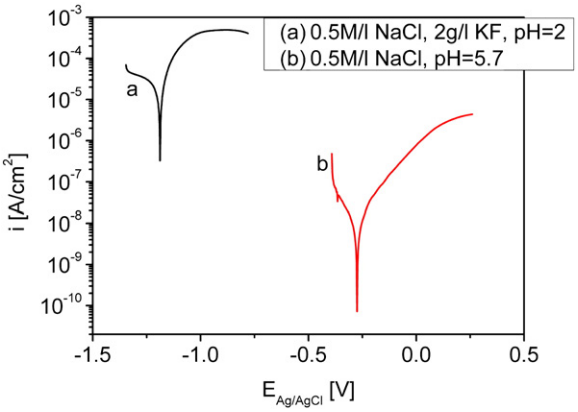

Fig. 1. Polarization curves of titanium alloy in 0.5 M/l NaCl, pH = 5.7; 0.5 M/l NaCl, 2 g/l KF, pH = 2.4.

the metal. This passive layer isolates the surface, resulting in a decrease of corrosion current.

Titanium and titanium alloys belong to a group of high-reactive materials, which is indicated by its relatively negative reversible potential on the electromotive force scale ($E^0 = -1.63$ V_{NHE}, NHE—normal hydrogen electrode). As a result of its reactivity, metallic titanium readily oxidized during exposure to air as well as during exposure to aqueous electrolytes. Oxidation leads to the formation of protective layer consisting mainly of titanium oxides: TiO_2 on the metal surface or Ti_2O_3 and TiO on metal/oxide interface. The presence of a protective layer of oxides on metal surface is a formidable barrier to corrosion processes [3]. However, in the presence of aggressive anion species, especially fluoride ions F^-, the oxide layer is not sustainable [4,5]. Also, the protective properties of the titanium oxide layer decrease with the decrease of pH [6]. All this leads to a significant increase in the rate of corrosion processes, expressed by an increase of corrosion current from 0.01 μA/cm² in neutral solution to 60.50 μA/cm² in acid solution containing fluoride ions. The change of corrosion potential depending on type of electrolyte also was observed. In neutral NaCl E_{corr} was −0.275 V, while for the acid solution with F^- ions $E_{corr} = -1.188$ V. In 0.5 M/l NaCl, 2 g/l KF, pH = 2 solution the corrosion potential was more negative, so the closer to the potential of pure metal titanium.

The described above corrosion mechanism causes destruction of the TiO_2 film passivity and loss of mechanical properties [7].

These characteristics limit the possibility of using the titanium alloys. Therefore, many various surface treatment techniques are used, to improve titanium and its alloys mechanical properties like surface hardness, wear resistance etc. and its corrosion properties. These methods include, burnishing and surface micro-shot peening and thermochemical treatment, in particular based on the PVD and CVD methods [8–10].

One way to protect titanium alloy surface from corrosion and improve its surface mechanical properties is application of oxide coatings. The oxide films lead to the metal surface insulation from environmental stress and, at the same time, cause improvement of the mechanical properties of the titanium alloy surface [11].

Another way to improve titanium alloys surface properties can be by graphene layer deposition. Graphene is one of the most inspiring and promising materials studied in recent years. It is composed of a single layer of carbon atoms forming six-membered rings linked together [12]. Studies have shown that a single graphene layer considerably increases the corrosion resistance of such systems as copper/graphene and nickel/graphene [14] and protects the surface of those metals from oxidation [13].

In this work structural, mechanical and corrosion properties of three different systems have been investigated and compared: Nb_2O_5/Ti–Al–V, Nb_2O_5:Cu/Ti–Al–V and graphene/Ti–Al–V. The niobium oxide (Nb_2O_5) layer and niobium oxide doped with copper (Nb_2O_5:Cu) layer have been chosen because of their high corrosion and wear resistance [15].

Table 1
Influence of the electrolyte composition on the electrochemical parameters of the Ti6Al4V titanium alloy obtained from polarization curves.

Electrolyte	i_{corr} [μA/cm²]	E_{corr} [V]
0.5 M/l NaCl, pH = 5.7	0.01	−0.275
0.5 M/l NaCl, 2 g/l KF, pH = 2	60.50	−1.188

Table 2
Composition of Ti6Al4V titanium alloy.

Components, wt.%						
C	Fe	N	O	Al	V	Ti
0.08	0.25	0.05	0.20	5.50–6.75	3.5–4.5	Bal

2. Experimental

For the purpose of the experiment, four sets of titanium alloy Ti6Al4V (ASTM Grade 5, UNS R56400) (Table 2) were prepared in the same manner. Before technological processes the titanium discs (25 mm in diameter and 4 mm thick) were polished using Stuers RotoPol-21 polishing machine and diamond suspension with 9, 3 and 1 μm grain size, respectively up to a roughness of 50 nm. Afterward, the polished discs were ultrasonically cleaned using acetone and ethanol solutions.

2.1. Nioba and nioba with copper thin film preparation and structural characterization

Thin films were prepared by magnetron sputtering method. An innovative multitarget apparatus was used for the deposition process [16]. This system allows for deposition of composite coatings from up to four targets. In this work, metallic niobium and copper targets were sputtered in a pure oxygen atmosphere and the working pressure during the sputtering was equal to ca. 3×10^{-3} mbar. The thickness of deposited thin films was measured with a Taylor Hobson Talysurf CCI Lite optical profilometer and was equal to 210 nm.

The elemental composition as well as images of the surface of the prepared thin films was obtained with the aid of a FESEM FEI Nova NanoSEM 230 scanning electron microscope equipped with an EDAX detector. The distribution of each element in the thin film with copper addition was also investigated.

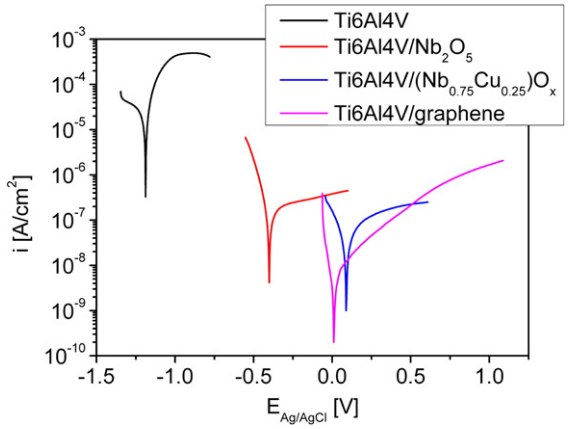

Fig. 2. Polarization curves of titanium alloy samples covered by thin film of Nb_2O_5, thin film of $(Nb_{0.75}Cu_{0.25})O_x$ and graphene monolayer, in 0.5 M/l NaCl, 2 g/l KF, pH = 2.4.

Table 3
Electrochemical parameters of the samples obtained from polarization curves in 0.5 M/l NaCl, 2 g/l KF, pH = 2 electrolyte solution.

Sample	i_{corr} [μA/cm^2]	E_{corr} [V]
Ti6Al4V	60.50	−1.188
Ti6Al4V Nb_2O_5	0.24	−0.401
Ti6Al4V $(Nb_{0.75}Cu_{0.25})O_x$	0.07	0.010
Ti6Al4V/graphene	0.01	0.011

To determine the surface topography properties before and after the corrosion process, the AFM (Atomic Force Microscopy) measurements were performed by the UHV VT AFM/STM Omicron atomic force microscope operating in ultra high vacuum conditions in the contact mode.

2.2. Graphene layer preparation and structural characterization

The graphene monolayers were grown on 18-μm thick copper foil using chemical vapor deposition (CVD) technique. For this purpose a home-made CVD set based on Blue M Tube Furnace with a 1-inch diameter reactor tube was used. During the growth process the reactor chamber is set at low pressure (~10^{-6} Torr) and heated up to ~1000 °C in a hydrogen atmosphere. Methane is used as a carbon source (growth time is typically 10 min).

Graphene was transferred onto the titanium alloy substrate using "PMMA-mediated" method [17]. First, PMMA (495 K, about 100 nm thick) was spin-coated on top of the synthesized graphene on copper substrate and dried for 24 h at room temperature. Next, the graphene from bottom of Cu substrate was etched by reactive ion etching method in oxygen plasma (PlasmaLab 80+, Oxford Instruments). After that, the exposed Cu foil was dissolved in an aqueous etchant of iron (III) nitrate for several hours. When the copper is dissolved the graphene sample was cleaned in DI (deionized) water. Next, ion particle removing step was used with hydrochloric acid solution, hydrogen peroxide as catalyst dissolved in water [17]. After all cleaning steps PMMA/graphene layer was transferred on titanium alloy substrate and annealed in order to evaporate the water and increase adhesion between graphene and the surface. In the last step the PMMA layer was removed.

The quality and number of transferred layers were evaluated by Raman spectroscopy (InVia Renishaw Spectrometer, 514 nm laser line, standard and streamline mode). All Raman spectra were collected at room temperature using 1 mW of laser power (on the sample).

The quality of the graphene monolayer transferred onto the titanium alloy surface before and after corrosion process, was investigated by AFM measurements.

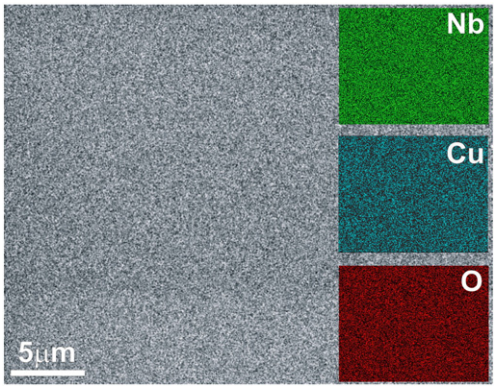

Fig. 3. Results of X-ray microanalysis showing secondary electron image with Nb, Cu and O elements distribution in the $(Nb_{0.75}Cu_{0.25})O_x$ thin film.

2.3. Mechanical and electrochemical characterization

The hardness measurements of the obtained coatings were performed with a nanoindenter manufactured by CSM Instrument equipped with a diamond Vickers indenter. The compound hardness was calculated using the method proposed by Oliver and Pharr [18]. Each data point represents an average of five indentations. A number of measurements were carried out for various depths of nanoindentation (from 80 nm to 700 nm). In order to measure the "film-only" properties and minimize the impact of the substrate a method of nanoindentation measurements approximation was implemented [19]. Measured hardness of the thin films deposited on substrate can be expressed as a power-low function of the substrate and the thin film hardness, the depth of nanoindentation and the thickness of thin film [19]:

$$H = H_S\left(\frac{H_f}{H_S}\right)^M \tag{1}$$

where: H_s—hardness of substrate, H_f—hardness of thin film, and M—dimensionless spatial function defined by [20]:

$$M = \frac{1}{1 + A(h/d)^B} \tag{2}$$

where: A, B—adjustable coefficients, h—maximum intender displacement, and d—thickness of thin film.

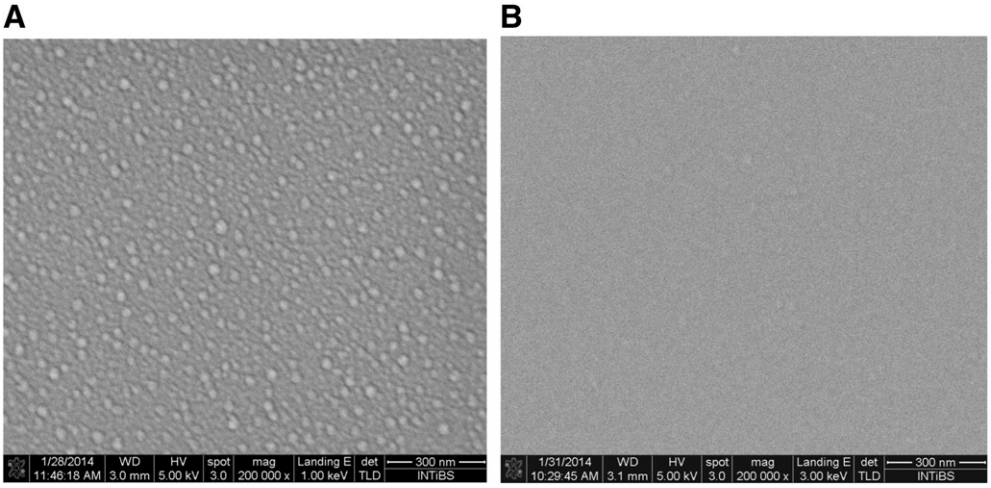

Fig. 4. Results of the measurements of Nb_2O_5 and $(Nb_{0.75}Cu_{0.25})O_x$ thin films by SEM.

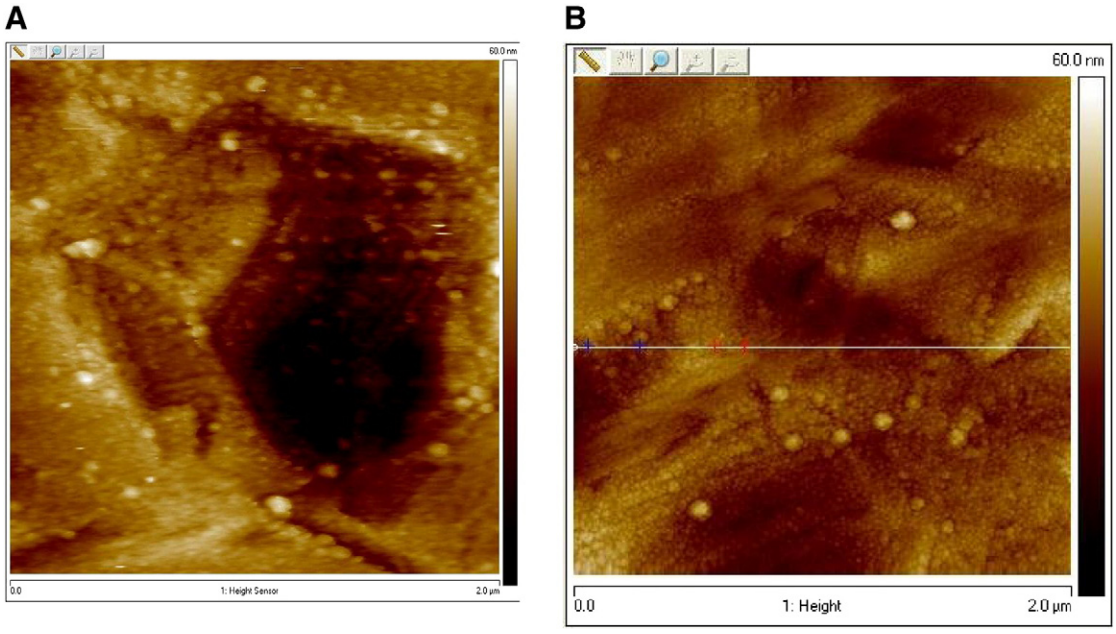

Fig. 5. Results of the measurement of Nb_2O_5 thin film; (A) before and (B) after corrosion process by AFM.

Eq. (1) must fulfill essential boundary conditions: when indentation depth approaches zero (small indentation displacements) measured hardness tends to thin film hardness. Whereas when indentation depth approaches the thin film thickness, measured hardness tends to the value of the substrate hardness.

Electrochemical measurements were carried out in 0.5 M/l NaCl, 2 g/l KF, pH = 2 solution adjusted by concentrated hydrochloric acid. Voltametric measurements (polarization curves) were carried out with a scan rate of 1 mV/s within the range of −150 mV to 1000 mV versus open circuit potentials and polarization curves corresponding to every examined material were recorded. Prior to each polarization experiments, the samples were immersed in the electrolyte for 1 h while monitoring the open circuit potential to establish steady state conditions. A three-electrode cell arrangement was applied using the Ag/AgCl electrode with Luggin capillary as reference electrode and a platinum wire as the auxiliary electrode (counter electrode). The measurements were carried out by means of Autolab EcoChemie System of AUTOLAB PGSTAT 302 N type equipped with GPESv. 4.9. software in aerated solutions at room temperature. The values of corrosion current densities (i_{corr}) were obtained from the polarization curves by extrapolation of the cathodic and anodic branch of the polarization curves to the corrosion potential [21].

3. Results and discussion

3.1. Corrosion properties

Fig. 2 presents polarization curves of titanium alloy and titanium alloys with deposited undoped niobia thin film, niobia with copper addition thin film and graphene monolayer in 0.5 M/l NaCl, 2 g/l KF, pH = 2

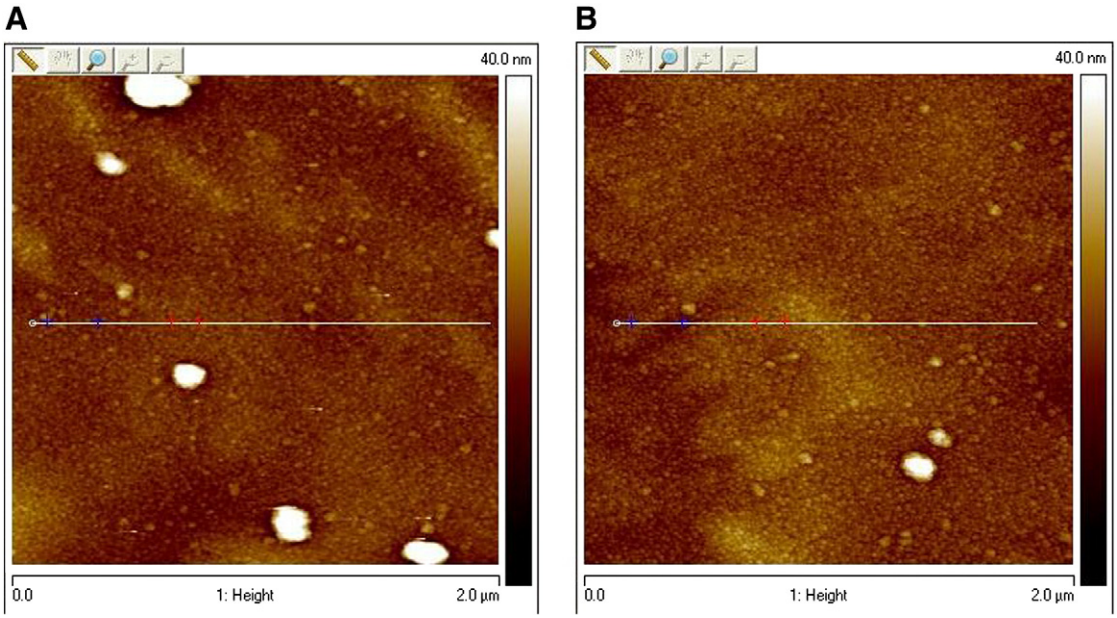

Fig. 6. Results of the measurement of $(Nb_{0.75}Cu_{0.25})O_x$ thin film (A) before and (B) after corrosion process by AFM.

electrolyte solution. The thin films on the surface of titanium alloy caused a significant decrease in the value of corrosion current densities (i_{corr}) (Table 3).

The best corrosion properties (the smallest corrosion current density) were obtained for sample Ti6Al4V with graphene monolayer ($i_{corr} = 0.01\ \mu A/cm^2$). The presence of graphene monolayer on the surface of titanium alloy also resulted in changes in the value of corrosion potentials E_{corr} (Table 3).

Corrosion properties of the tested thin films Nb_2O_5 and $(Nb_{0.75}Cu_{0.25})O_x$ on the surfaces of titanium alloy depend on composition of the thin layer. Addition of copper (i.e. noble metal) to Nb_2O_5 film increases the corrosion resistance followed by a significant decrease in the value of corrosion current density and caused the shift of corrosion potential towards noble direction. The shift of the corrosion potential in the noble direction decreases the electrochemical activity of the surface and improves its corrosion resistance. Similar results were obtained for the samples covered by graphene monolayer and $(Nb_{0.75}Cu_{0.25})O_x$ layer (210 nm).

3.2. Structural properties of niobium pentoxide and niobium pentoxide with copper thin films before and after corrosion process

Material composition of thin films was measured using energy dispersive spectroscopy and the amount of copper addition was equal to 25 at.% without taking into consideration the signal of oxygen from the measurements. Therefore, in this paper coating with copper addition is denoted as $(Nb_{0.75}Cu_{0.25})O_x$. Additionally, exemplary result of X-ray microanalysis of $(Nb_{0.75}Cu_{0.25})O_x$ thin film (Fig. 3) showed, that the distribution of each investigated element (Nb, Cu, O) is homogenous. The area of investigation was ca. 32 mm × 25 mm.

In Fig. 4A–B SEM images of the surface of the investigated thin films are shown. The deposited coatings were crack free and exhibited good

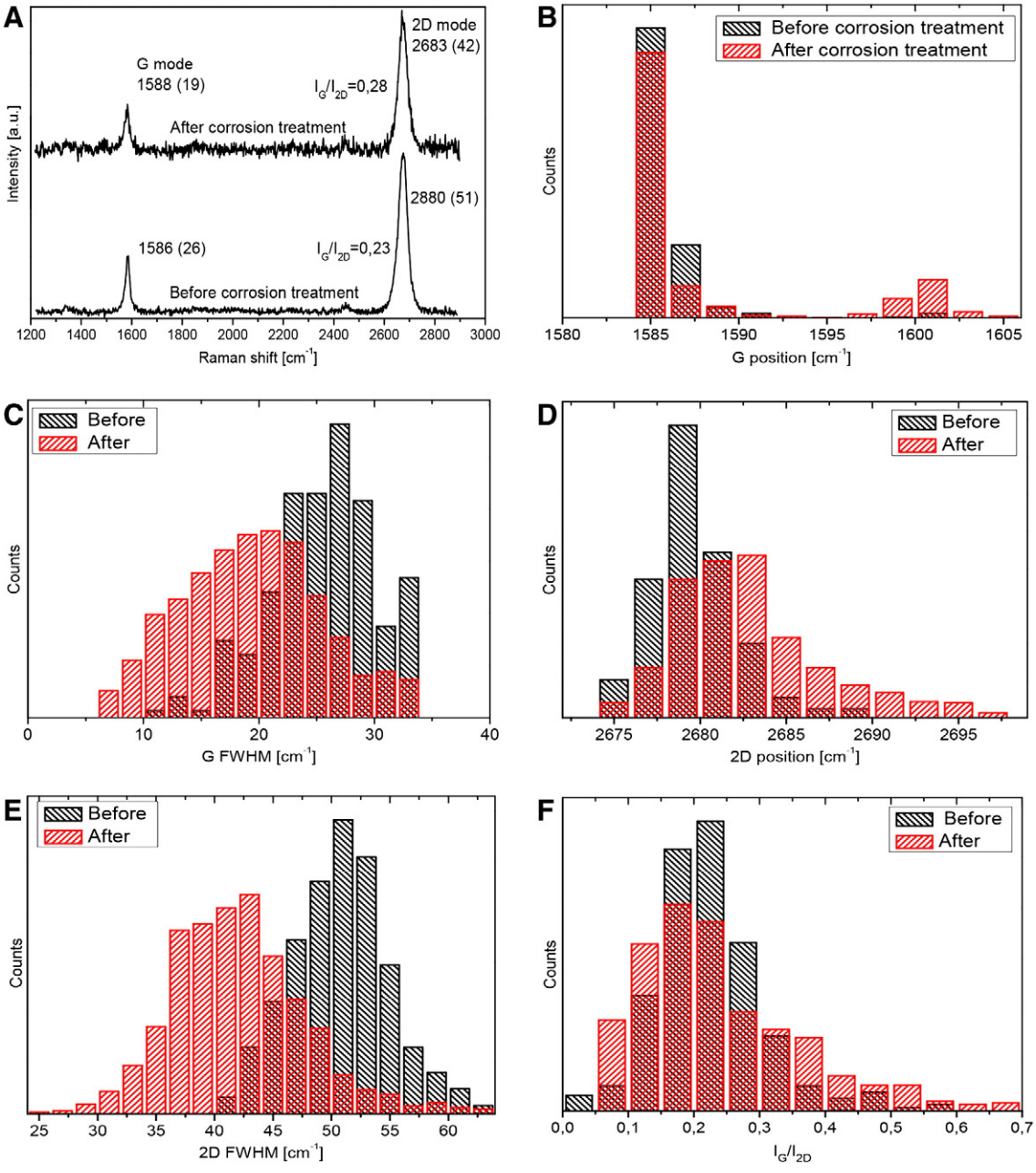

Fig. 7. The statistical analysis of Raman spectra obtained for graphene/Ti–Al–V system before and after corrosion process.

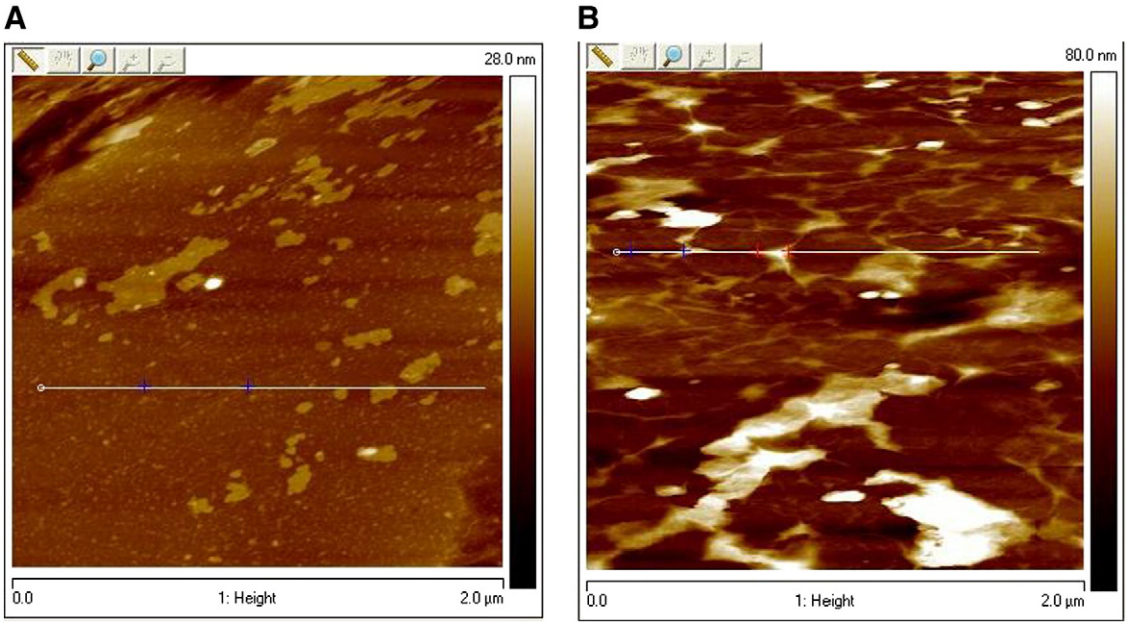

Fig. 8. Results of the measurement of graphene monolayer (A) before and (B) after corrosion process by AFM.

adherence to the substrate, no discontinuities of the thin film were observed and the surface morphology was homogeneous. The particles are visible in the image of undoped niobia thin film and have a uniform shape (Fig. 4A). Addition of copper to the nioba coating resulted in the significant change of surface properties i.e. no particles are visible in the SEM images (Fig. 4B).

AFM measurements were performed in order to extend the information about the surface topography of the as-prepared thin films before and after corrosion process. The AFM images are shown in Figs. 5 and 6. In the case of undoped niobia, the surface before (Fig. 5A) and after corrosion (Fig. 5B) process is crack-free and densely packed.

After the corrosion process it is clearly seen, that small organic molecules form a passive layer on the top of the thin Nb_2O_5 film (Fig. 5B). This passive layer blocks-out the intrinsic porosity of the coating, leading to decreased corrosion current value [22–24].

In the case of $(Nb_{0.75}Cu_{0.25})O_x$ thin film, the surface was more flat and homogenous as-compared to undoped niobia (compare Figs. 5A and 6A). The surface properties were not changed after the corrosion process (compare Fig. 6A and B). In this case probably, the passive film is formed much slower than in the case of pure nioba film and is denser. It is probably related to the homogeneous nature of the $(Nb_{0.75}Cu_{0.25})O_x$ thin film [22]. Confirmation of this thesis can provide the results obtained from electrochemical measurements. The results show, that the $(Nb_{0.75}Cu_{0.25})O_x$ thin film, provides better barrier against corrosion than Nb_2O_5 thin film.

3.3. Structural properties of graphene/Ti–Al–V system before and after corrosion process

Raman spectroscopy is a nondestructive and fast method for the study of various carbon materials. In case of graphene, Raman spectra give information about the number of layers [25], material quality and defects [26,27]. Typical Raman spectra consist of 3 main modes: D mode (~1350 cm^{-1}), G mode (~1580 cm^{-1}) and 2D mode (~2700 cm^{-1}). Monolayer graphene sheet is easily identified by Raman study simply by looking at the G/2D relative intensity ratio (usually about 0.2), also taking into account the shape of those peaks [25]. The quality of graphene sheet can be verified by the appearance of D mode peak, usually taken as the relative ID/IG ratio [26,28].

Fig. 7A shows the comparison of graphene/Ti–Al–V Raman spectra collected before and after the corrosion process. It is clearly seen that after the corrosion process of graphene/Ti–Al–V system, the graphene Raman signature is almost unchanged suggesting that graphene is a corrosion-resistant layer. Importantly, the D mode (~1350 cm^{-1}) is not seen in the spectra after corrosion process, which proves that graphene has been not damaged in the process and it is acting as shield for the Ti–Al–V surface.

More information about how much influence the corrosion process has on our system is seen in the statistical analysis of approximately 900 Raman spectra. Statistics of the positions show that the G mode

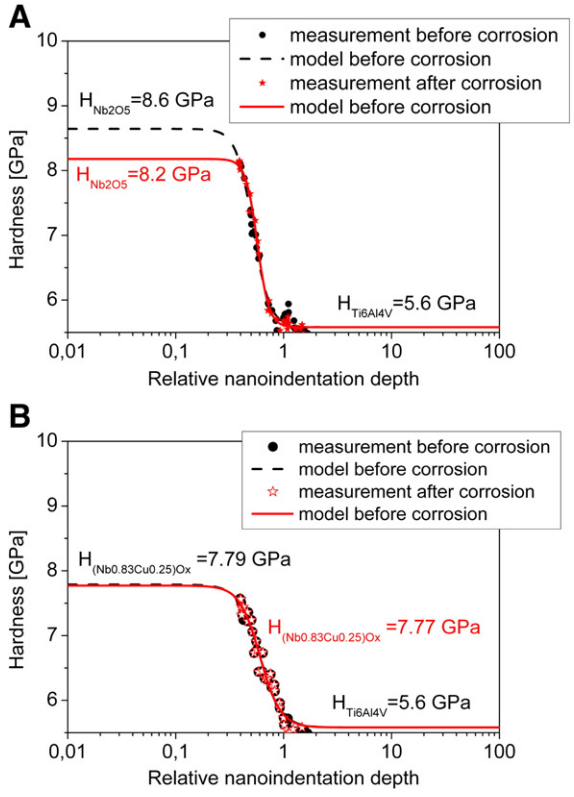

Fig. 9. Results of hardness investigation for Nb_2O_5, $(Nb_{0.75}Cu_{0.25})O_x$ thin film before and after corrosion process.

Table 4
Hardness value obtained from nanoindentation measurements before and after corrosion process.

	Ti6Al4V	Ti6Al4V/Nb_2O_5	Ti6Al4V/$(Nb_{0.75}Cu_{0.25})O_x$	Ti6Al4V/graphene
$H_{before\ corrosion}$ [GPa]	5.64	8.64	7.79	5.63
$H_{after\ corrosion}$ [GPa]	4.95	8.16	7.77	5.62

(Fig. 7B) after the corrosion process exhibits splitting and upshift (~1585 and 1601 cm^{-1}). The 2D band position also exhibits slight upshift after the corrosion process (Fig. 7D). This suggests either strong graphene doping in some areas or lower local heating upon laser exposure (due to the cleaner surface). The down shift of full width at half maximum (FWHM) for both main Raman bands (Fig. 7C and E) clearly confirms that the corrosion process acts as a cleaning process of the graphene layer, removing all contaminant (e.g. Fe3 + ions that left after copper etching in transfer process) from the surface leaving graphene intact. Interestingly, the relative intensity ratio of the G and 2D modes remains the same after corrosion measurement. This confirms that the uniformity of monolayer graphene structure is preserved.

In Fig. 8A–B the AFM images for Ti–Al–V/graphene system, are shown. It is clearly seen, that after the corrosion process (Fig. 8B), the regions in the gaps changed color (white); thus it indicates that those regions formed an oxide layer [29].

However, the titanium alloy regions under the graphene flakes are still pristine and shiny, which indicates that these regions are not oxidized. We could clearly see the flakes under the color contrast [29]. The titanium alloy regions located under graphene flakes are better protected than regions located under the gaps.

3.4. Mechanical properties before and after corrosion process

The hardness of the titanium alloy and prepared niobium pentoxide layer, $(Nb_{0.75}Cu_{0.25})O_x$ layer and graphene monolayer has been measured by nanoindentation. For the first two types of the layers nanohardness has been determined by approximation method. For pure titanium alloy and titanium alloy covered by graphene monolayer, nanohardness has been measured at a constant depth equal 80 nm. It is the smallest depth, for which correct results have been obtained.

Hardness obtained for uncoated titanium alloy and titanium alloy covered by graphene monolayer, was equal to 5.64 GPa and 5.63 GPa, respectively and 8.64 GPa for Nb_2O_5 layer (Fig. 9A) and 7.79 GPa for $(Nb_{0.75}Cu_{0.25})O_x$ layer (Fig. 9B). As compared to the results presented in the literature reports, the hardness of investigated Nb_2O_5 thin film is higher of ca. 50% [30], 53% [31] and 46% [32]. After addition of copper into the Nb_2O_5 layer, its hardness decreased of about 10% from 8.64 GPa for Nb_2O_5 to 7.79 GPa for $(Nb_{0.75}Cu_{0.25})O_x$ layer, but it is still higher than the results presented in the literature reports for pure nioba layer.

Graphene layer deposited on titanium alloy surface is practically not seen by nanoindenter during measurements. Therefore, the measurement did not reveal changes of titanium alloy surface hardness after graphene deposition, in comparison with pure titanium alloy, and was equal to 5.63 GPa.

Nanoindentation measurements, performed after the corrosion process, show no change of surface hardness for $(Nb_{0.75}Cu_{0.25})O_x$ thin film and graphene monolayer. Only in the case of Nb_2O_5 thin film, decrease of surface hardness is observed. However, this change is still smaller, than that observed for pure titanium alloy.

Hardness obtained for pure nioba thin film after the corrosion process was equal to 8.16 GPa (Fig. 9A), for nioba with 25 percent copper addition: 7.77 GPa (Fig. 9B) and for titanium alloy surface covered by graphene monoloayer: 5.62 GPa (Table 4). For comparison, for uncovered titanium alloy, surface nanohardness decreases to the value of 4.95 GPa (Table 4) after the corrosion process. The value of surface hardness decreased by 13% as compared to the value obtained for uncovered titanium alloy before the corrosion process.

In the case of Nb_2O_5 thin film, decreasing of surface nanohardness after corrosion process, can be due to the passive layer formed on the top of the thin film during corrosion process [22–24]. Changes on the surface of uncovered titanium alloy, influenced by the corrosion process, capable of altering the surface hardness, are known and described in [33].

The observed differences in the value of the layers hardness, before and after corrosion process (0.02 GPa for nioba with 25 percent copper and 0.01 GPa for titanium alloy surface covered by graphene monolayer), were very small and within the extended uncertainty of nanohardness measurements with a confidence level of 95% and coverage factor k = 2, estimated at 0.2 GPa, for measurement range between 1 GPa and 9 GPa. Therefore, they are not regarded as changes in the hardness of the layers. The change in hardness value above 0.2 GPa, like in the case of not covered titanium alloy and Nb_2O_5 thin film, indicates the real change in the measured hardness of the material.

4. Summary

Obtained results have shown that niobium pentoxide layer, $(Nb_{0.75}Cu_{0.25})O_x$ layer and graphene monolayer deposited on titanium alloy surfaces, can be considered as barrier coatings for the Ti6Al4V alloy, to effectively protect its surface against corrosion processes, which take place on pure titanium alloy surface in very aggressive environments. Instead, only the Nb_2O_5 layer and $(Nb_{0.75}Cu_{0.25})O_x$ layer improved titanium alloy mechanical properties i.e.: surface hardness and wear resistance. However, from these three selected systems, only $(Nb_{0.75}Cu_{0.25})O_x$/Ti–Al–V system and graphene/Ti–Al–V system did not change mechanical properties (hardness) of titanium alloy surface during corrosion process.

It appears advisable to perform a combination of two types of coatings with a hybrid system, which improves mechanical and corrosion properties of the titanium alloy surface, and keeps the stability of this parameters during corrosion process. The proposed hybrid system consists of a mechanical resistance niobium pentoxide or $(Nb_{0.75}Cu_{0.25})O_x$ layer and graphene monolayer, which is characterized by very high corrosion resistance.

In the next order we will be evaluating the durability of corrosion and mechanical properties during the temporary exposure in corrosive environments: artificial saliva, SBF etc., and biocompatibility.

Acknowledgments

This work was financed by the National Centre for Research and Development in the years 2013–2016 as a research project no. GRAFTECH/NCBR/14/26/2013 “InGrafTi”.

References

[1] C.P. Dillon, Mater. Perform. 7 (1998) 69.
[2] R. Strietzel, A. Hosch, Biomaterials 19 (1998) 1495.
[3] J.R. Goldberg, J.L. Gilbert, Biomaterials 25 (5) (2004) 851.
[4] M. Nakagawa, T. Shiraishi Matsuya, M. Ohta, J. Dent. Res. 78 (9) (1999) 1568.
[5] R.W. Schutz, D.E. Thomas, Corrosion of Titanium and Titanium Alloys9th ed., Metals handbook, vol. 13, American Society for Metal (ASM) International, Metals Park, OH, 1987. (669).
[6] L. Kinani, A. Chtaini, Leonardo J. Sci. 12 (11) (2007) 33.
[7] M. Lorenzetti, E. Pellicer, J. Sort, M. Dolors Baró, J. Kovač, S. Novak, S. Kobe, Materials 7 (2014) 180.
[8] Y. Song, Z. Zhao, F. Lu, J. Mater. Sci. 1 (1) (2014) 17.
[9] S. Thamizhmnaii, B. Bin Omar, S. Saparudin, S. Hasan, J. Achiev. Mater. Manuf. Eng. 28 (2) (2008) 139.

[10] K.-T. Rie, Th. Lampe, Mater. Sci. Eng. 69 (2) (1985) 473.
[11] X. Liua, P.K. Chub, Ch. Dinga, Mater. Sci. Eng. R 47 (2004) 49.
[12] http://zadniwiedzy.pl/.
[13] V. Mišković-Stanković, I. Jevremović, I. Jung, K.Y. Rhee, Carbon 75 (2014) 335.
[14] D. Prasai, ACS Nano 6 (2012) 1102.
[15] M. Mazur, M. Kalisz, D. Wojcieszak, M. Grobelny, P. Mazur, D. Kaczmarek, J. Domaradzki, Mater. Sci. Eng. C 47 (2014) 211.
[16] D. Kaczmarek, J. Domaradzki, B. Adamiak, J. Dora, S. Maguda, Polish patent application2011. P396389.
[17] X. Liang, B.A. Sperling, I. Calizo, G. Cheng, C.A. Hacker, Q. Zhang, Y. Obeng, K. Yan, H. Peng, Q. Li, X. Zhu, H. Yuan, A.R. Hight Walker, Z. Liu, L. Peng, C.A. Richter, ACS Nano 5 (2011) 11.
[18] W.C. Oliver, G.M. Pharr, J. Mater. Res. 7 (1992) 1564.
[19] Y.-G. Jung, B.R. Lawn, M. Martyniuk, H. Huang, X.Z. Hu, J. Mater. Res. 19 (2004) 3076.
[20] B.V. Crist, Handbook of the Elements and Native Oxides, XPS International Inc., Iowa, USA, 1999.
[21] F. Mansfeld, ASM Handbook, 13A, ASM International, 2003. 446.
[22] P.N. Rojas, S.E. Rodil, Int. J. Electrochem. Sci. 7 (2012) 1443.
[23] I. Arsova, A. Prusi, T. Grcev, L. Arsov, J. Serb. Chem. Soc. 71 (2006) 177.
[24] D.B. Camovska, M.Lj. Arsov, T.p. Grcev, Maced. J. Chem. Chem. Eng. 26 (2007) 95.
[25] A. Gupta, G. Chen, P. Joshi, S. Tadigadapa, P.C. Eklund, Nano Lett. 6 (2006) 12.
[26] A. Jorio, M.S. Dresselhaus, R. Saito, G. Dresselhaus, Raman Spectroscopy in Graphene Related Systems, Wiley-VCH, Weinheim, Germany, 2011.
[27] V. Singh, D. Joung, L. Zhai, S. Das, S.I. Khondaker, S. Seal, Prog. Mater. Sci. 56 (2011) 1178.
[28] A.C. Ferrari, J.C. Meyer, V. Scardaci, C. Casiraghi, M. Lazzeri, F. Mauri, S. Piscanec, D. Jiang, K.S. Novoselov, S. Roth, A.K. Geim, Phys. Rev. Lett. 97 (2006) 187401.
[29] X. Zhou, Graphene Oxidation Barrier CoatingThesis April 2011.
[30] G. Ramírez, S.E. Rodil, S. Muhl, D. Turcio-Ortega, J.J. Olaya, M. Rivera, E. Camps, L. Escobar- Alarcón, J. Non-Cryst. Solids 356 (50-51) (2010) 2714.
[31] J.M. Chappé, P. Carvalho, S. Lanceros-Mendez, M.I. Vasilevskiy, F. Vaz, A.V. Machado, M. Fenker, E. Alves, Surf. Coat. Technol. 202 (11) (2008) 2363.
[32] C. Eda, B. Baloukas, O. Zabeida, J.E. Klemberg-Sapieha, L. Martinu, Appl. Opt. 48 (23) (2009) 4536.
[33] Titanium alloy guide, RMI Titanium Company. An RTI International Metals, Inc. Company, January 2000.